

# The Measurement of Plasma Structure in a Magnetic Thrust Chamber<sup>\*</sup>)

Ryosuke KAWASHIMA, Taichi MORITA<sup>1)</sup>, Naoji YAMAMOTO<sup>1)</sup>, Naoya SAITO, Shinsuke FUJIOKA<sup>2)</sup>, Hiroaki NISHIMURA<sup>2)</sup>, Hiraku MATSUKUMA<sup>2)</sup>, Atsushi SUNAHARA<sup>3)</sup>, Yoshitaka MORI<sup>4)</sup>, Tomoyuki JOHZAKI<sup>5)</sup> and Hideki NAKASHIMA<sup>1)</sup>

Department of Advanced Energy Engineering Science, Kyushu University,  
6-1 Kasuga-Koen, Kasuga, Fukuoka 816-8580, Japan

<sup>1)</sup>Faculty of Engineering Sciences, Kyushu University, 6-1 Kasuga-Koen, Kasuga, Fukuoka 816-8580, Japan

<sup>2)</sup>Institute of Laser Engineering, Osaka University, 2-6 Yamadaoka, Suita, Osaka 565-0871, Japan

<sup>3)</sup>Institute for Laser Technology, 1-8-4 Utsubo-honmachi, Nishi-ku, Osaka 550-0004, Japan

<sup>4)</sup>The Graduate School for the Creation of New Photonics Industries, Hamamatsu 431-1202, Japan

<sup>5)</sup>Faculty of Engineering, Hiroshima University, Higashi-Hiroshima 739-8527, Japan

(Received 31 July 2015 / Accepted 3 November 2015)

Magnetic thrust chamber is a propulsion system controlling plasma by a magnetic field and is expected as a propulsion system of laser fusion rocket. This rocket obtains thrust due to the interaction between plasma and magnetic field in the system. We examine the plasma structure in a magnetic thrust chamber by observing the light emission from the plasma with several magnetic field strength. The experiments imply that anisotropic plasma expansion is induced by the applied magnetic field and the velocity is decreased at the magnetic field above 0.67 T.

© 2016 The Japan Society of Plasma Science and Nuclear Fusion Research

Keywords: laser fusion rocket, magnetic thrust chamber, plasma, magnetic field, plasma emission

DOI: 10.1585/pfr.11.3406012

## 1. Introduction

Laser Fusion Rocket (LFR) is a spaceship utilizing an extravagant amount of nuclear fusion energy and controlling fusion plasma with an external magnetic field. LFR has a potential to produce large thrust and high specific impulse simultaneously, so that it is expected as a rocket of interplanetary missions [1].

In interplanetary missions, long duration of the exposure of cosmic ray and living in an enclosed space deteriorate both physical and mental health of astronauts, and reducing mission period is indispensable. LFR is expected to solve this issue because of its potential to generate large thrust. In addition, the thruster can control the exhaust mass and velocity with wide range so that it enables an optimal design of the thruster depending on missions [2, 3]. In this paper, such a thruster is called “Magnetic Thrust Chamber”.

The mechanism of thrust generation in a magnetic thrust chamber is shown in Fig. 1. Plasma expands as shown in Fig. 1 (a). The plasma induces a diamagnetic current to sweep aside the magnetic field and magnetic field is compressed [Fig. 1 (b)]. The compressed magnetic field pushes back the plasma and the spaceship obtains the thrust as a reaction force as described in Fig. 1 (c).

author's e-mail: kawashima@aes.kyushu-u.ac.jp

<sup>\*</sup>) This article is based on the presentation at the Conference on Laser Energetics 2015 (CLE2015).

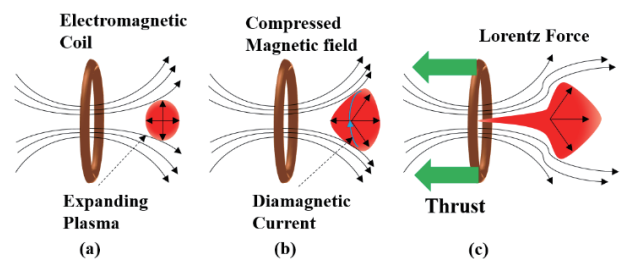


Fig. 1 The mechanism of thrust generation of magnetic thrust chamber. (a) Laser irradiates a target pellet to generate nuclear reaction. The fusion plasma expands in a magnetic field generated by electromagnetic coil. (b) The plasma induces a diamagnetic current to sweep aside the magnetic field and magnetic field is compressed. (c) The compressed magnetic field pushes back the plasma and the spaceship is accelerated by the reaction.

In previous researches, a magnetic thrust chamber has been studied with numerical simulations and laser experiments. Nagamine *et al.* have simulated a plasma behavior in magnetic field using a three-dimensional (3D) hybrid code, treating ions as particles and electrons as fluid, respectively [4]. Maeno *et al.* combined a one-dimensional (1D) radiation hydrodynamic code with a 3D hybrid code to simulate the creation process of a laser-produced plasma [5]. In addition, they examined the effect of the magnetic

field strength on a plasma behavior [6]. Some experiments in laser facilities with the energy of 4 J to 1 kJ have been performed. Maeno *et al.* have directly measured thrust generated by a magnetic thrust chamber [7]. Yasunaga *et al.* have examined the interaction between magnetic field and laser-produced plasma, and observed the diamagnetic cavity [8]. However, the plasma structure in a magnetic thrust chamber has never been observed experimentally.

In this paper, we examine the plasma structure in a magnetic thrust chamber by observing the light emission of a laser-produced plasma with several magnetic field strength. We observed the plasma deceleration.

## 2. Characteristics of Plasma Expansion

Nikitin *et al.* have discussed the dynamics of the 3D expansion of a spherical cloud of rarefied plasma into a vacuum in the presence of a dipole magnetic field, in the framework of ideal MHD approximation. They described how to determine the configuration and location of the plasma front which is caused by the retardation effect [9]. In addition, they defined parameter that characterizes the interaction between the expanding plasma and the dipole field,

$$\kappa = \frac{E_p}{E_M} = \frac{12\pi E_p R_0^3}{\mu_0 |\mu_d|^2},$$

where  $E_p$  is the kinetic energy of ions,  $E_M$  is the field energy integrated beyond the spherical radius  $R_0$  ( $E_M = (\mu_0/4\pi)|\mu_d|^2/(3R_0^3)$ ).  $R_0$  is the distance from the magnetic coil to the initial target position.  $\mu_0$  is the vacuum magnetic permeability and  $|\mu_d|$  is the magnetic moment magnitude. The critical value  $\kappa_c$  was found by Nikitin *et al.* for different plasma locations. When  $\kappa$  is lower than  $\kappa_c$ , substantial plasma deceleration will occur in all directions from the explosion location. (When the plasma is located on the axis of the magnetic field as in this experiment, the critical value is  $\kappa_c = 0.4$ .) [10].

## 3. Experimental Setup

The experiment was performed at the Extreme Ultraviolet (EUV) database facility of the Institute of Laser Engineering (ILE) in Osaka University. The experimental setup is shown in Fig. 2. A plasma was created by focusing a 1064-nm Neodymium: Yttrium Aluminum Garnet (Nd:YAG) laser onto a polystyrene ( $[-\text{CH}_2-\text{CH}(\text{C}_6\text{H}_5)-]_n$ ) spherical target with a diameter of 500  $\mu\text{m}$ . The pulse width of laser is  $9.5 \pm 0.5$  ns and the laser energy is  $6.0 \pm 0.8$  J. The target is suspended by a carbon fiber attached to a glass rod to reduce the plasma formation of glass rod. The distance between the coil surface and the target is 13 mm.

Magnetic field was generated by flowing current into a 96-turn electromagnetic coil with the inner radius of 13 mm and outer radius of 25 mm. The current was gener-

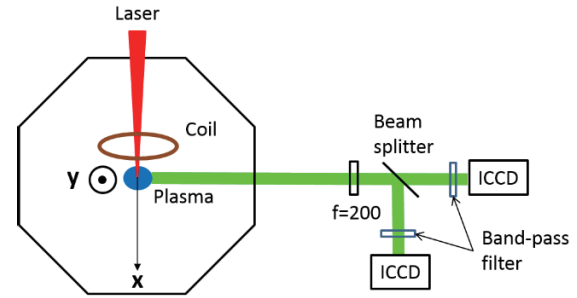


Fig. 2 Experimental setup. YAG laser irradiated the target and generated the plasma. The laser energy was  $6.0 \pm 0.8$  J, pulse width is  $9.5 \pm 0.5$  ns and the wavelength was 1064 nm. The emission from the plasma was recorded with ICCD cameras through a band pass filter and lens ( $f = 200$  mm).

Table 1 Parameter  $\kappa$  in several magnetic field strength.

The magnetic field strength [T]	$\kappa$
0.12	3.3
0.23	0.67
0.46	0.17
0.67	0.077
0.89	0.044
1.1	0.029

ated by a capacitor bank, in which three 32 mF capacitors were connected in parallel. The magnetic field of 1.1 T was generated at the initial target position by applying 500 V on the capacitor bank.

We also calculated as shown in Table 1, implying that plasma deceleration would occur over 0.46 T ( $\kappa < \kappa_c = 0.4$ ). In our experiment,  $E_p = 6$  J (We assume almost 100% of laser energy is converted to the kinetic energy of ions [11].),  $R_0 = 13$  mm, and  $\mu_d = 11, 24, 48, 72, 94,$  and  $116 \text{ A}\cdot\text{m}^2$  with the magnetic field strength of 0.12, 0.23, 0.46, 0.67, 0.89, and 1.1 T, respectively.

The emission from the plasma was collected with a lens (focal length of 200 mm) and imaged onto intensified charge coupled devices (ICCDs) at a wavelength of 660 nm with a band-path filter with the width of 10 nm (FWHM). Two ICCDs were used to take images of different delay times in a single laser-shot. The self-emission recorded here is composed of H-alpha and thermal bremsstrahlung emissions.

## 4. Result and Discussion

Figure 3 shows the initial magnetic field configuration generated by the electromagnetic coil.

Figures 4 (a) - 4 (f) show the light emission from the plasma with the magnetic field of 0, 0.23, 0.46, 0.67, 0.89, and 1.1 T, respectively, at  $1.0 \mu\text{s}$  after plasma generation. In these figures, the target was set at the coordinate  $(x, y) = (0, 0)$  and was irradiated with the laser from left side through the hole of the coil. The center axis of the

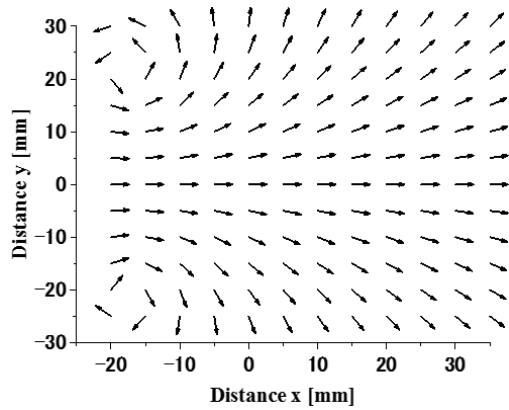


Fig. 3 Initial magnetic field configuration generated by electromagnetic coil.

magnetic field corresponds to the  $x$ -axis at  $y = 0$ .

Without the magnetic field, the plasma expands to  $-x$  direction and  $\pm y$  directions.

With the magnetic field, the plasma expansion to  $-x$  and  $\pm y$  direction is suppressed by the magnetic field. Comparing the plasma emission in  $+y$  direction with that in  $-y$  direction, the plasma intensities in  $+y$  direction is higher than that in  $-y$  direction. Since the high-energy plasma hit the carbon fiber attached to a glass rod, the fiber is ablated and the ablation plasma emits light.

Figure 5(a) shows the light intensities from the plasma averaged from  $y = -4$  to  $4$  mm along the  $x$ -axis at  $1.0 \mu\text{s}$  in Figs. 4(a) - 4(f) with six different magnetic field strength. Without magnetic field, a peak of plasma intensity at  $x = -10$  mm shows the plasma generated by

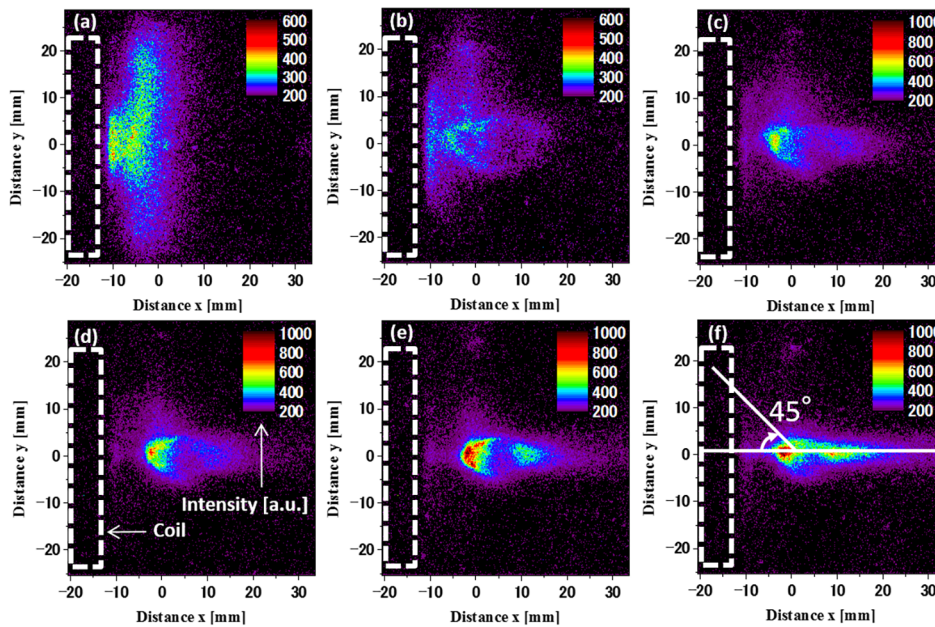


Fig. 4 The light emission from the plasma (a) without and with the magnetic field of (b) 0.23 T, (c) 0.46 T, (d) 0.67 T, (e) 0.89 T, and (f) 1.1 T at  $1.0 \mu\text{s}$  after laser irradiation. In these figures, target was set at the coordinate  $(x, y) = (0, 0)$  and was irradiated with the laser from left side through the hole of the coil.

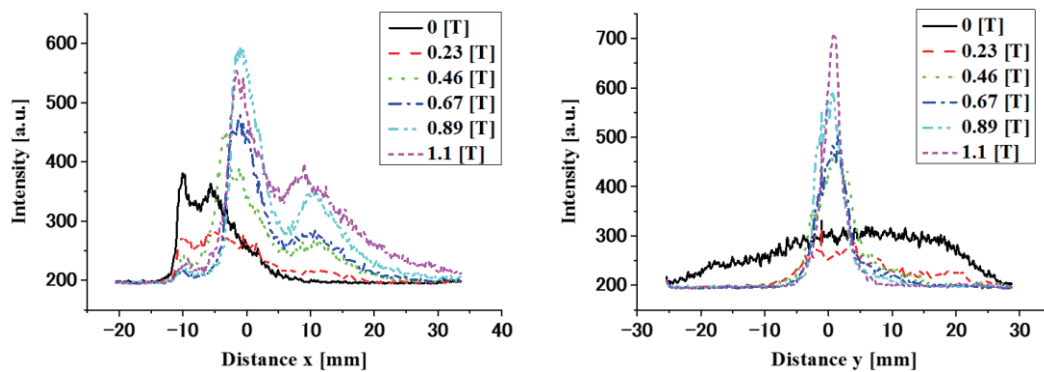


Fig. 5 (a) The light intensities from the plasma averaged from  $y = -4$  to  $4$  mm along the  $x$  direction at  $1.0 \mu\text{s}$  in Figs. 4(a) - 4(f). The light intensity in  $x$  direction is higher as magnetic field strength is larger. (b) The light intensities from the plasma averaged from  $x = -5$  to  $0$  mm along the  $y$  direction at  $1.0 \mu\text{s}$  in Figs. 4(a) - 4(f). The width with magnetic field is smaller than that without magnetic field.

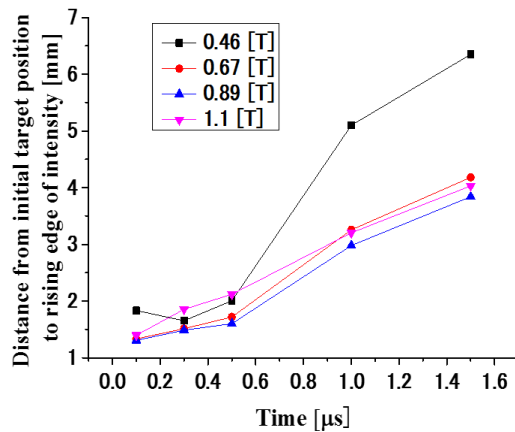


Fig. 6 Distance from initial target position  $(x, y) = (0, 0)$  to rising edges of the plasma intensity with several magnetic field strength as a function of time.

the laser-produced plasma from the target surface colliding with the coil surface. The light intensity in  $+x$  direction is higher as the magnetic field strength is larger. Figure 5 (b) shows the light intensities from the plasma averaged from  $x = -5$  to 0 mm along the  $y$  direction at 1.0  $\mu\text{s}$  in Figs. 4 (a) - 4 (f) with six different magnetic field strength. The width of plasma expansion to  $\pm y$  direction with magnetic field is smaller than that without magnetic field. The intensity at  $x = 0$  is higher as magnetic field strength is larger. This shows the plasma is suppressed by the magnetic field in  $y$  direction and does not expand across the magnetic field.

We examined the distance from initial target position  $(x, y) = (0, 0)$  to rising edge of plasma intensity along the direction of  $45^\circ$  from  $x$ -axis as shown in Fig. 4 (f). We assumed the rising edge of plasma intensity shows the interaction between the expanding plasma and the magnetic field. Figure 6 gives plots of the distance as a function of time with several magnetic field strength. Figure 6 indicates the deceleration of plasma in the magnetic field over 0.67 T because the distance from initial target position to rising edge of the plasma intensity with 0.46 T is larger than that with over 0.67 T. As for 0.67 T,  $\kappa$  value of 0.077 is much smaller than the critical value  $\kappa_c = 0.4$  because the plasma is ejected only in laser irradiation side and  $\kappa_c = 0.4$  is overestimated in the present experiment. This indicates that the larger magnetic field with small  $\kappa$  is required to decelerate the plasma.

In the future plan, we will examine thrust efficiency and compare the results of experiment with simulation re-

sults to realize Laser Fusion Rocket. Experimental investigations on a thrust efficiency and the comparison between numerical and experimental analyses will be our future work. Nagamine *et al.* [5] examined thrust efficiency as a function of criterion  $E_B/E_p$ . Here,  $E_B$  is the magnetic field energy and represented by  $E_B = 1/2LI^2$  ( $L$ : Inductance [ $\mu\text{H}$ ],  $I$ : Current [ $\text{A}$ ]).  $E_p$  is the initial plasma kinetic energy. They found thrust efficiency is the maximum when  $E_B$  is five times greater than  $E_p$ . In a conceptual laser fusion rocket VISTA [1], a value of 5 is adopted for the ratio.

## 5. Conclusion

We measured the plasma emission with and without an external magnetic field to investigate the interaction between plasma and a magnetic field in a magnetic thrust chamber. The plasma expansion in both  $-x$  and  $\pm y$  directions is suppressed by the magnetic field. In addition, the light intensity in  $+x$  direction is higher as magnetic field strength is larger. Therefore, the plasma expands to  $+x$  direction more, which contributes to obtain thrust as the magnetic field strength is larger. We also calculated the criterion and confirmed the plasma deceleration in a magnetic field over 0.67 T.

## Acknowledgement

Authors would like to thank Mr. Eiji Sato for his exceptional support during this experiment. This work was supported by the Japan Society for the Promotion of Science (JSPS) KAKENHI (Grant Numbers 25420852 and 15K18283) and by the joint research project of the Institute of Laser Engineering, Osaka University (2014B1-31).

- [1] C.D. Orth *et al.*, UCRL-TR-110500 (2003).
- [2] S. Uchida, J. Plasma Fusion Res. **81**, 186 (2005) (in Japanese).
- [3] S. Uchida, Plasma Fusion Res. **83**, 271 (2007) (in Japanese).
- [4] Y. Nagamine *et al.*, Fusion Technol. **35**, 62 (1999).
- [5] A. Maeno *et al.*, Trans. JSASS Aerospace Tech. Japan **10**, 28, 71 (2012).
- [6] A. Maeno *et al.*, J. Propul. Power **30**, 1, 54 (2014).
- [7] A. Maeno *et al.*, Appl. Phys. Lett. **99**, 071501 (2011).
- [8] M. Yasunaga *et al.*, Trans. JSASS Aerospace Tech. Japan **10**, 28, 109 (2012).
- [9] S.A. Nikitin and A.G. Ponomarenko, J. Appl. Mech. Tech. Phys. **34**, 745 (1993).
- [10] K.V. Vchivkov *et al.*, Jpn. J. Appl. Phys. **42**, 6590 (2003).
- [11] C. Yamanaka, Laser Engineering (Corona, Inc., 1981) p.106-168 (in Japanese).